Charge Injection and STM-Induced Vacancy Migration on GaAs(110)

G. Lengel, J. Harper, and M. Weimer
Department of Physics, Texas A&M University, College Station, Texas 77843-4242
(Received 28 December 1995)

Migration of anion and cation vacancies on GaAs(110) has been examined with scanning tunneling microscopy. Striking asymmetries are found in the direction and bias-polarity dependence of the migration probability that signal the importance of both bonding topology at the surface and bulk doping. These asymmetries indicate vacancy motion is driven by recombination of carriers injected via the STM tip with carriers from the bulk. The impact-parameter dependence of the reaction cross section shows this injection occurs through resonant tunneling into dangling-bond defect states. [S0031-9007(96)00043-9]

PACS numbers: 61.16.Ch, 68.35.Dv, 68.35.Fx

Manipulation of individual atoms at surfaces with the scanning tunneling microscope (STM) has evolved from a visionary conception [1] to a technologically significant reality [2,3] in less than a decade, yet despite remarkable progress in elucidating many of the fundamental physical principles involved in these and related processes [4–13], much remains unknown.

Here we consider a phenomenon closely related to atomic manipulation, the STM-induced migration of surface defects [14–16]. We have noted distinctive asymmetries in both the crystallographic-direction and bias-polarity dependence of the migration probability for anion and cation vacancies on GaAs(110) that point to a new mechanism—minority carrier injection by the STM tip—as the physical stimulus that catalyzes vacancy motion. Using the unique spatial resolution available with STM, we are able to identify a critical reaction coordinate and to map out the impact-parameter dependence of the migration cross section. The data are consistent with a picture in which resonant tunneling of minority carriers into dangling-bond defect states is followed by recombination to provide the energy necessary to drive vacancy motion. This mechanism, though specific to the surface, shares many features with a well-documented phenomenon in bulk semiconductors: the recombination enhanced defect reaction [17–19]. Such reactions are of practical importance since they are thought to promote the degradation of quantum-well lasers [20]. Our findings also complement recent suggestions concerning the significant role that resonant processes play in STM-induced adsorbate reactions at metal and semiconductor surfaces [11,13,21].

The experiments reported in this Letter utilized both *p*- and *n*-doped GaAs wafers since As vacancies occur on degenerate *p*-type samples (and are positively charged), whereas Ga vacancies occur on degenerate *n*-type samples (and are negatively charged) [22]. These wafers were cleaved in UHV ($\leq 5 \times 10^{-11}$ torr) to expose a fresh (110) surface. Standard bias voltages of $+2.5$, -2.0 V and $+2.0$, -2.5 V were employed for atom-selective imaging [23] on *p*- and *n*-type material, respectively, with setpoint currents ≤ 100 pA. The crystal orientation and scanning directions were systematically varied.

Vacancy migration is recognized by the appearance of a "split" defect in the STM scans [15,22], as illustrated in Fig. 1. In this example, the tip is rastered from the lower left to the upper right. While moving toward the right, the sample (in this case *p*-type) is negatively biased so that electrons tunnel out of the filled As dangling bonds; while moving back toward the left along each horizontal scan line, the sample is positively biased so that electrons then tunnel into empty Ga dangling-bond states. A missing atom in the As image, together with a pair of symmetrically relaxed neighbors in the Ga image, identifies an As vacancy [24]. As the vacancy is approached from below, it jumps to a neighboring site twice during this frame—first along a zigzag chain, and then across to another chain—so that each time an atom rather than a vacancy is imaged in the next

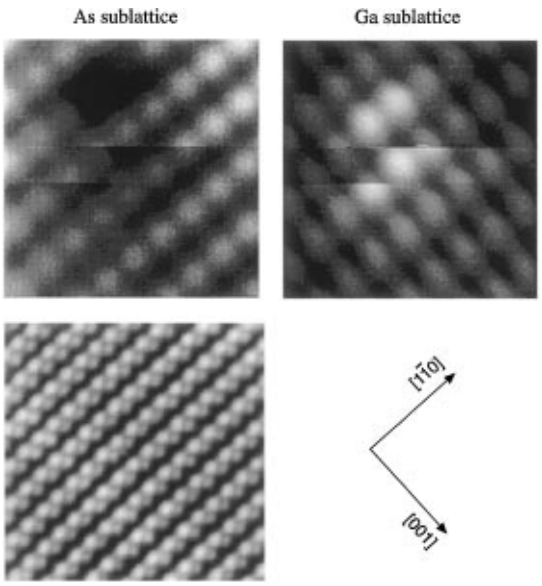

FIG. 1. Top: Simultaneously-acquired images illustrating successive migrations of an As vacancy. Bottom: Composite of As (white) and Ga (gray) sublattices.

 © 1996 The American Physical Society

As line. Complementary features identify Ga vacancy motion on *n*-GaAs when the roles of anion and cation are interchanged.

A total of 349 migration events (264 As vacancy, 85 Ga vacancy) gathered from 35 different samples (15 *p*-type, 20 *n*-type) were analyzed for this study. The orientation of the crystal axes for each sample was established from each sample from the pairing of As and Ga atoms into $[1\bar{1}0]$ zigzag chains, as shown in Fig. 1. In this particular instance, the initial and final locations of the defect were recorded for both migration events, and the corresponding directions of vacancy motion are therefore known. If a vacancy originates from a region just ahead of the tip, however, or moves behind it into an area that was already scanned, its direction of motion cannot be determined from a single pair of simultaneously-acquired images, and the event is classified as "unknown."

The direction dependence of vacancy migration is summarized in Table I. Two points are evident from the table: First, motion of anion vacancies between the surface zigzag chains ([001] direction) is much more common than motion along the chains ($[1\bar{1}0]$ direction) [25]; migration of cation vacancies, on the other hand, is more nearly isotropic. This difference presumably arises from the inequivalence of anion and cation geometries at the relaxed GaAs(110) surface, where arsenic atoms sit above the bulk termination plane and gallium atoms are pushed down into the bulk. Second, if we focus on either vacancy alone, we see that interchain translation is *unidirectional* with respect to a (001) plane: Arsenic vacancies translate in the $[00\bar{1}]$, but not the $[001]$ direction, whereas the opposite is true of gallium vacancies. This striking fact—illustrated for As vacancies in Fig. 2—reflects the absence of (001) mirror symmetry at the (110) surface.

The unidirectional character of interchain migration on GaAs(110) is undoubtedly related to the way in which bonds are broken and reformed during vacancy motion. If an anion or cation vacancy moves in a given direction, a corresponding surface atom must move in the opposite direction. Referring again to Fig. 2, we see that the As atom immediately to the right of a vacancy must initially break two surface bonds to jump into the empty sublattice site. The As atom immediately to the left, however, need only break a single back bond, and then swing up and over its Ga neighbors—in a natural, rigid-bond rotation that preserves two surface bonds throughout its trajectory—before rebonding and dropping back down to fill in the defect [25]. While time-reversal symmetry demands a unique height for the energy barrier, irrespective of whether motion is to the left or to the right, the bonding topology at the surface will certainly influence the barrier's shape. The irreversibility of interchain migration thus rules out any thermally-activated process that depends *only* on the barrier height, and points to a nonequilibrium, inelastic mechanism instead.

In most instances, the bias polarity and tip location associated with a given migration event can also be determined, as illustrated with the As vacancy in Fig. 3. The scan sequence here is the same as in Fig. 1, but the frame is rotated by 90° so that the [001] axis now points toward the upper right. This example (which falls into the "unknown" category mentioned above) displays a characteristic discontinuity in the Ga image (line 25) that is an unmistakable indication of the moment and conditions under which migration occurred. The preceding line (line 24) demonstrates the familiar relaxation of the neighboring Ga atoms. These atoms abruptly return to their normal positions (creating the discontinuity in line 25) when the original vacancy is filled. The temporally bracketing As lines (25, 26) show that the defect just "disappears" from this image.

The bias-polarity dependence of vacancy migration reveals two additional asymmetries [26]: First, we find that As vacancies migrate only when *electrons*, and not holes, are injected into the surface. Second, it appears Ga vacancies migrate only when *holes*, and not electrons, are injected. It is important to appreciate these conclusions are based on an equivalent sampling of the two directions of current flow that was independently assured for each

TABLE I. Direction dependence of vacancy migration.

Crystallographic direction	As vacancy	Ga vacancy
$[00\bar{1}]$	108	0
[001]	0	21
$[1\bar{1}\bar{2}]$ or $[\bar{1}1\bar{2}]$	78	0
$[1\bar{1}2]$ or $[\bar{1}12]$	0	22
$[1\bar{1}0]$ or $[\bar{1}10]$	17	20
Unknown	61	22

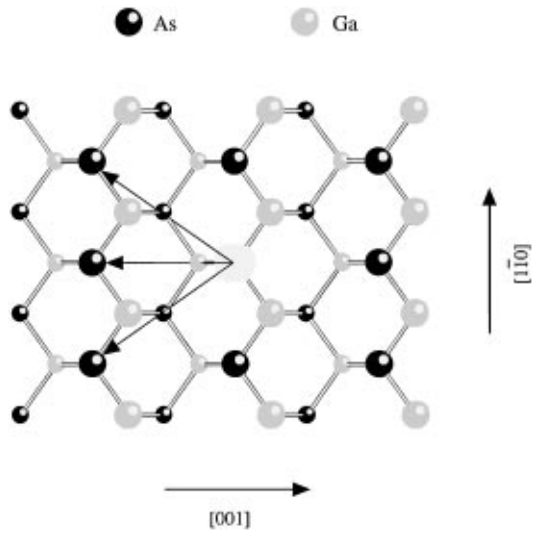

FIG. 2. Schematic view of the GaAs(110) surface. Large circles represent surface atoms, and small circles atoms in the second layer. Arrows emphasize interchain migration is unidirectional with respect to a (001) plane.

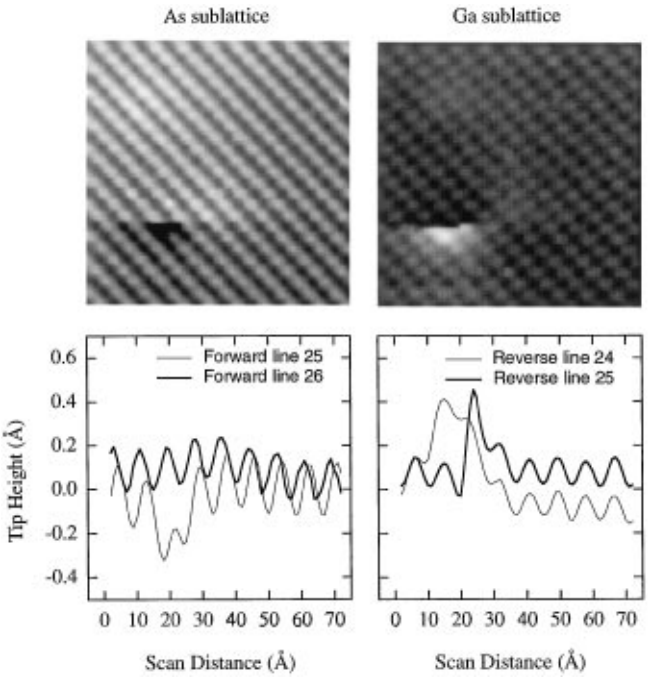

FIG. 3. Top: Simultaneously-acquired images of a single migration event. Bottom: Successive scan lines from each image, offset for clarity.

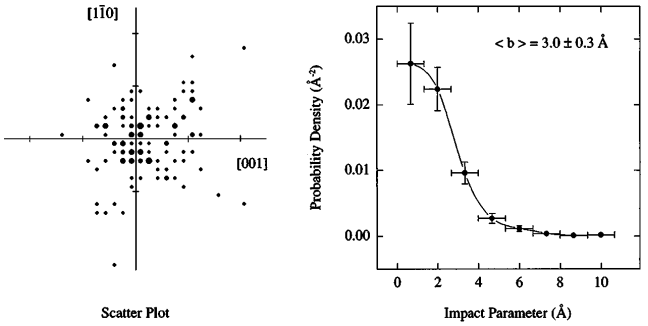

FIG. 4. Left: Scatter plot illustrating the locus of carrier injection that stimulates As vacancy migration on *p*-GaAs. Crystal axes, centered on the vacancy and oriented as in Fig. 2, are marked in units of the appropriate lattice constant. Symbol size is proportional to the number of events at each location. Right: Probability density for migration as a function of impact parameter. Solid line is a spline fit.

defect by analyzing only simultaneously-acquired pairs of anion and cation images.

A scatter plot illustrating the relative coordinates of the migration pixels for As vacancies is shown in Fig. 4. The distribution is essentially isotropic, and nearly all of the events are clustered within a region bounded by the eight neighboring surface As sites. Reducing this two-dimensional plot to a one-dimensional dependence on lateral distance from the origin yields the probability density for vacancy migration as a function of the tip's impact parameter, $(1/N)(dN/2\pi bdb)$, also shown in Fig. 4. We find a mean impact parameter of 3.0 ± 0.3 Å, and see that electron injection must occur within $\sim$6 Å of an As vacancy if there is to be any appreciable chance of stimulating a migration event. The comparable radial distribution for Ga vacancies, though not as strongly peaked, is also localized on an atomic scale.

The vacancy motion described here is clearly stimulated by the STM tip. As we now argue, however, the physical mechanism responsible for this phenomenon is distinctly different from those previously invoked to explain the manipulation of individual atoms with the STM. For example, short-range bonding that results in mass transfer between tip and sample [7,9] requires a two-step process in which atoms are first deposited on and then removed from the surface (or vice versa) and this is inconsistent with our empirical finding that the vacancy structure is always preserved during migration (Fig. 1). Local heating due to multiple inelastic vibrational excitation is possible only when the associated relaxation times are long [10], and there is no reason to suspect this is the case for substrate atoms whose modes are strongly coupled to the bulk. Electrostatic phenomena [4] such as field desorption and field-enhanced diffusion are inconsistent with the bias-polarity dependence and locality of migration. Combining the information on the direction of current flow with the clustering of migration pixels seen in the scatter plots (Fig. 4), we conclude that negatively (positively) charged As (Ga) anions (cations) almost always move toward—rather than away from—negatively (positively) charged tips, whereas positively (negatively) charged tips have no effect. Similar reasoning shows that the forces on surface dipoles [4,5], which arise from cation-to-anion charge transfer, also have the wrong sign, while induced polarization forces should be independent of bias polarity.

Barrier lowering due to the electric field of the tip [9] is likewise unimportant for two reasons. First, this phenomenon occurs at the maximum of the migration barrier, which should lie somewhere *between* the original defect and the backbond of the atom that subsequently moves to fill it in (Fig. 2). As Fig. 4 clearly shows, however, migration is most probable when the tip is centered over the vacancy and not at all likely when the tip is over this bond. Second, and more significant, is the observation that the effect of barrier lowering is to increase the thermal probability for barrier crossing. As we have already remarked, such a process is inconsistent with the unidirectional character of interchain migration.

We believe the key to understanding vacancy migration on GaAs(110) lies in the relationship between the direction of current flow associated with defect motion and the bulk doping: Since As and Ga vacancies are found on *p*- and *n*-type samples, respectively, the carriers that are injected by the STM tip when migration occurs are *minority* carriers in either case. These excess carriers may be introduced directly into mid-gap vacancy levels, where they will change the charge state of the defect, or they can go into the bulk bands.

It appears there are only two routes whereby charge injection can lead to defect motion: either through barrier

lowering or through recombination. A significant lowering of the barriers for vacancy migration due to a change in charge state [27] is suspect for essentially the same reasons described above in connection with the tip's electric field. Here, however, the clustering of migration pixels shown in Fig. 4 is interpreted as evidence this injected charge goes into localized dangling bonds associated with the vacancy, and not into states that govern the bonding of neighboring atoms (Fig. 2).

Defect-mediated recombination of minority carriers injected by the tip with majority carriers from the bulk, on the other hand, will liberate an energy comparable to a single bond-breaking event in GaAs. That energy is available to assist migration provided there is large lattice distortion, or strong electron-phonon coupling, associated with a change in occupancy of the defect levels [17–19].

We can assess the relevance of this bulk picture to our experiments by reexamining the probability density for vacancy migration illustrated in Fig. 4. That quantity is proportional to the square of a quantum-mechanical transition amplitude [28] and thus depends on the integrated overlap of initial and final state wave functions with a perturbation Hamiltonian for carrier capture. One expects the perturbation, which arises from the vacancy charge, to have a range of order the Debye screening length ($\sim$15 Å) whereas the wave function associated with a deep defect center will be localized on the scale of a lattice constant ($\sim$6 Å). An electron captured from within a few k_BT ($\sim$100 meV) of the conduction band edge, on the other hand, will have a spatial extent in excess of 25 Å by virtue of the uncertainty principle, and this spread is inconsistent with the short-ranged impact-parameter dependence observed in Fig. 4.

There is a related picture, specific to the surface, however, that accounts for the complementary bias asymmetries exhibited by *p*- and *n*-type samples as well as a mean impact parameter of the order of atomic dimensions. In this mechanism, vacancy migration is initiated by resonant tunneling of minority carriers directly into dangling-bond defect states where they then recombine with band-edge majority carriers. Precise details concerning the way in which that recombination energy is channeled into a normal coordinate for migration—for example, whether the electron-lattice coupling is adiabatic or nonadiabatic [29,30]—are not yet clear in this case, but the same chemical arguments used to rationalize the (001) asymmetry of interchain migration strongly suggest at least one of these coordinates is associated with a localized "rocking" mode of the buckled surface zigzag chains [31,32]. The relative importance of single- versus multiple-carrier [10,11] excitation is also not presently known.

Lower bounds on the inelastic cross section for this process may be found from the mean number of vacancy jumps and the energy-integrated carrier density delivered by the tip. This flux-time product ($\sim 1.0 \times 10^6$ Å^{-2}) was varied through half a decade by changing the dwell time per unit area rather than the feedback current, and the relative probability of multistep migration sequences (Fig. 1) increased with the incident carrier density. Resulting estimates of the reaction cross section are $\sigma_{\mathrm{As}} > 4 \times 10^{-22}$ cm^2 and $\sigma_{\mathrm{Ga}} > 3 \times 10^{-23}$ cm^2, respectively, consistent with either radiative or nonradiative recombination at deep centers [29,30]. Whether these differing probabilities for anion and cation vacancy migration reflect the energy dependence of the resonant injection, the nature of the subsequent recombination, or the migration barriers themselves remains an open question.

We have benefited from discussions with a number of colleagues but especially wish to thank V. Pokrovsky, A. L. Ford, and R. E. Allen. This work was supported by grants from the Office of Naval Research and the Robert A. Welch Foundation.

[1] R. S. Becker *et al.,* Nature (London) **325**, 419 (1987).
[2] J. W. Lyding *et al.,* Appl. Phys. Lett. **64**, 2010 (1994).
[3] C. T. Salling and M. G. Lagally, Science **265**, 502 (1994).
[4] J. A. Stroscio and D. M. Eigler, Science **254**, 1319 (1991).
[5] L. J. Whitman *et al.,* Science **251**, 1206 (1991).
[6] D. M. Eigler *et al.,* Nature (London) **352**, 600 (1991).
[7] I.-W. Lyo and P. Avouris, Science **253**, 173 (1991).
[8] G. Dujardin *et al.,* Science **255**, 1232 (1992).
[9] N. D. Lang, Phys. Rev. B **45**, 13 599 (1992).
[10] R. E. Walkup *et al.,* Phys. Rev. B **48**, 1858 (1993).
[11] G. P. Salam *et al.,* Phys. Rev. B **49**, 10 655 (1994).
[12] B. N. J. Persson and P. Avouris, Chem. Phys. Lett. **242**, 483 (1995).
[13] T.-C. Shen *et al.,* Science **268**, 1590 (1995).
[14] S. Gwo *et al.,* J. Vac. Sci. Technol. A **11**, 1644 (1993).
[15] P. Ebert *et al.,* Phys. Rev. Lett. **70**, 1437 (1993).
[16] T. Nakayama *et al.,* Surf. Sci. **320**, L101 (1994).
[17] J. D. Weeks *et al.,* Phys. Rev. B **12**, 3286 (1975).
[18] C. H. Henry and D. V. Lang, Phys. Rev. B **15**, 989 (1977).
[19] H. Sumi, Phys. Rev. B **29**, 4616 (1984).
[20] F. A. Houle *et al.,* J. Appl. Phys. **72**, 3884 (1992).
[21] B. N. J. Persson and A. Baratoff, Phys. Rev. Lett. **59**, 339 (1987).
[22] G. Lengel *et al.,* J. Vac. Sci. Technol. B **11**, 1472 (1993).
[23] R. M. Feenstra *et al.,* Phys. Rev. Lett. **58**, 1192 (1987).
[24] G. Lengel *et al.,* Phys. Rev. Lett. **72**, 836 (1994).
[25] G. Lengel *et al.,* J. Vac. Sci. Technol. A **12**, 1855 (1994).
[26] G. Lengel *et al.,* J. Vac. Sci. Technol. B **13**, 1144 (1995).
[27] J. C. Bourgoin and J. W. Corbett, Phys. Lett. **38A**, 135 (1972).
[28] J. R. Taylor, *Scattering Theory* (John Wiley & Sons, Inc., New York, 1972).
[29] B. K. Ridley, *Quantum Processes in Semiconductors* (Clarendon Press, Oxford, 1988), 2nd ed.
[30] K. W. Boer, *Survey of Semiconductor Physics* (Van Nostrand Reinhold, New York, 1990).
[31] Y. R. Wang and C. B. Duke, Surf. Sci. **205**, L755 (1988).
[32] P. K. Das and R. E. Allen, in *The Physics of Semiconductors,* edited by E. M. Anastassakis and J. D. Joannopoulos (World Scientific, Singapore, 1990).